Identification and Characterization of a Biomineralization Related Gene PFMG1 Highly Expressed in the Mantle of *Pinctada fucata*†

Hai-Luo Liu,‡ Shang-Feng Liu,‡,§ Ye-Jing Ge,§ Jing Liu,‡ Xiao-Yan Wang,‡ Li-Ping Xie,§ Rong-Qing Zhang,§ and Zhao Wang*,‡,§

Medical School and Department of Biological Sciences and Biotechnology, Tsinghua University, Beijing 100084, People's Republic of China

Received September 10, 2006; Revised Manuscript Received October 24, 2006

ABSTRACT: To elucidate the mechanism of nacre biomineralization, the mantle of *Pinctada fucata* (*P. fucata*) from the South China Sea was used. Using the mantle cDNA library and the ESTs we have cloned through suppression subtractive hybridization (SSH), ten novel genes including PFMG1 were obtained through nested PCR. Bioinformative results showed that PFMG1 had a high homology (40%) with *Onchocerca volvulus* calcium-binding protein CBP-1 and had two EF-hand calcium-binding domains from the 81st to the 93rd amino acid and from the 98th to the 133rd amino acid in the deduced amino acid sequence. The results of multitissue RT-PCR and in situ hybridization demonstrated the high expression of PFMG1 in the mantle of *P. fucata* and confirmed the SSH method. The results of GST-PFMG1 on $CaCO_3$ crystallization showed significant effects on nucleation and precipitation of $CaCO_3$. PFMG1 was cloned into the pcDNA.3.1/myc-HisA vector and was subsequently transfected into MC3T3-E1 cells. RT-PCR revealed upregulation of the marker genes related to cell growth, differentiation, and mineralization, and BMP-2, osterix, and osteopontin were upregulated as a result. This research work suggests that PFMG1 plays an important role in the nacre biomineralization, and the SSH method can pave the way for the bulk cloning and characterization of new genes involved in biomineralization in *P. fucata* and may accelerate research on the mechanism of pearl formation.

As we know, pearl consists of nacre that is secreted by the mantle of the pearl oyster. Recent studies show that nacre may be an ideal substitute material for bone. It not only has a high rigidity but also has good biological adaptability and bone-inductive activeness. It can stimulate the growth of bone while not induce serious immunoreactions (*1*).

Pearl is a typical biomineralization product. It mainly consists of about 95% calcium carbonate and about 5% organic macromolecules.

Biomineralization is the process in which mineral crystals accumulate in an organized manner (*2*) under the control of organic macromolecules (*3*−*5*) (protein, amylose, etc.) excreted by the specific positions of living organisms, and the most significant characteristic is that the nucleation of the inorganic phase is strictly controlled by the organic phase (*6*). More than 60 kinds of products of biomineralization have been discovered, including pearls and shells of mollusks (*7*), spicula of poriferans, bones, teeth, kidney stones, and gallstones of vertebrates. More than half of them are calcium compounds.

The growth of molluscan nacre crystals is usually thought to initiate from solution by extracellular organic matrixes. Organic matrixes induce heterogeneous nucleation of calcium carbonate crystals on their surface and regulate crystal growth, thereby forming the crystal morphologies that are unique to the various layers of a molluscan shell. In vitro studies using natural and synthetic molecular systems have shown that matrix control of crystal morphology is possible (*8*−*11*).

One alternative to the current matrix mediation hypothesis presently is that crystal nucleation is intracellular and that crystallogenic cells supply nascent crystals to the mineralization front where they may undergo further growth and refolding (*12*). So we can conclude that the mechanism of biomineralization is not simply the mediation by the organic matrixes but a combination of nucleation, growth, morphology, recognition, transportation, and precipitation. Therefore, in order to fully understand the mechanism of biomineralization, it is necessary to find the key genes involved in biomineralization and take them as a whole in future studies.

Pinctada fucata (*P. fucata*)[1] grows in the South China Sea and Japanese Sea and is the main seashell yielding pearls with high economic value. For *P. fucata*, about ten correlative genes have been identified presently, including MSI31 (*13*), MSI60 (*13*), MSI7 (*14*), N16 (*15*) protein family, nacrein (*16*), pearlin (*17*), QM (*18*, *19*), calmodulin (*20*), prismalin-14 (*21*), and aspein (*22*). Also, there are reports on the cloning of genes of actin, ferritin (*23*), 18S ribosome, and G-protein (*24*). These genes play an important role in the

† This work was supported by the National High Technology Research and Development Program of China (2001AA621140), the National Natural Science Foundation of China (No. 30472162), the Tsinghua-Yue-Yuen Medical Sciences Fund (THYY20040008), and the China Postdoctoral Foundation (2004035052).

* Address correspondence to this author. Tel: +86-10-62772241. Fax: +86-10-62772240. E-mail: zwang@tsinghua.edu.cn.

‡ Medical School, Tsinghua University.

§ Department of Biological Sciences and Biotechnology, Tsinghua University.

10.1021/bi061881a CCC: $37.00
Published on Web 12/24/2006

performance of many significant life activities for *P. fucata*, but they have little to do with biomineralization. These genes are needed for comparison in studies on functional genes involved in biomineralization, and it is no doubt that the cloning of these genes will also lead to the further study of other functional genes.

In our research, *P. fucata*, the most important pearl oyster with pearl output accounting for more than 85% of the world, was used. We performed suppression subtractive hybridization (SSH) and reverse Northern dot blotting and obtained ESTs which are highly expressed in the mantle of *P. fucata*. The results should pave the way for the future cloning of new genes involved in biomineralization in *P. fucata*.

MATERIALS AND METHODS

Subtracted Library Construction by Suppression Subtractive Hybridization (25). Mantle tissue fragments from three live pearl mollusks (*P. fucata*, grows in Guangxi, China) were obtained. Total RNA was purified from mantle tissue fragments of *P. fucata* using the Trizol reagent (Invitrogen). Polyadenylated RNA was further isolated using Oligotex mRNA kits (Qiagen). The cDNA synthesis of mantle tissue (tester) and other tissues (driver) and SSH were performed using a PCR-select cDNA subtraction kit (Clontech) following the manufacturer's protocol. Briefly, tester and driver cDNA were digested separately with *Rsa*I to obtain shorter, blunt-ended molecules. The tester cDNA was divided into two populations, each of which was ligated with different adaptors provided in the kit, whereas the driver cDNA had no adaptors. Tester and driver cDNA were heated to 98 °C for 1.5 min, and each of the tester cDNA samples was separately hybridized with the driver at 68 °C for 8 h. The two hybridization mixtures were mixed without being denatured again. Additional denatured driver was added, and the mixture was hybridized for 16 h. After two rounds of hybridization as above, templates for PCR amplification were generated from differentially expressed sequences. Using two rounds of suppression PCR, differentially expressed sequences were enriched. The subtracted library cDNA (secondary PCR products) was cloned into the pGEM-T easy TA cloning kit (Promega) vector. DH5α cells were transformed. Bacterial cells were plated on LB agar plates containing 100 μg/mL ampicillin, 100 μM isopropyl 1-thio-β-D-galactopyranoside, and 50 μg/mL 5-bromo-4-chloro-3-indolyl β-D-galactopyranoside.

Reverse Northern Dot Blotting. For reverse Northern dot blotting experiments, 384 ampicillin-resistant clones were randomly picked from each plate and lysed by boiling in 50 mL of lysis buffer (0.1% Tween 20 in TE buffer, pH 8.0). The cloned cDNA fragments were amplified using primers flanking the cloning site of the vector. Each PCR product was dot-blotted onto duplicate nylon membranes using a microfiltration system. The membranes were UV cross-linked and probed with total (^{32}P)cDNA. The (^{32}P)cDNA probes were prepared using two rounds of suppression PCR.

Sequence Analysis. On the basis of the results of reverse Northern dot blotting, recombinant DNAs with expression 5 times higher in mantle than in other tissues were obtained and sequenced on a Model 377 automatic sequencing machine (PE) using T7 universal primer. The sequences were analyzed using Blast (NCBI) software, and the homology was compared with the sequences in GenBank.

Protein families and domains were determined using the PROSITE database at the ExPASy proteomics server of the Swiss Institute of Bioinformatics (http://www.expasy.org/prosite).

Construction of a Mantle Tissue cDNA Library. Total RNA was isolated from 0.5 g of mantle tissue using Trizol reagent (Invitrogen); then we synthesized first-strand cDNA catalyzed by reverse transcriptase (Sangon). Double-strand cDNA was synthesized following attachment of adaptors. The products were digested by *Sfi*I and then fractionated by gel filtration through Sepharose spin-400. The cDNA product was then cloned in the pBluescript II SK vector. Then we screened the library for desired clones and validated the identity of the clones.

Nested PCR Analyses (26). The PCR analyses were conducted through nested reactions using two pairs of outer primers (Sangon). The reaction mixtures were composed of 1.5 μg of cDNA, 200 μM each of four deoxynucleotide triphosphates along with $MgCl_2$ (2 mM), 10 × PCR buffer, and 1.25 units of DNA polymerase (Sangon). This reaction mixture was then denatured (90 s at 95 °C) followed by 35 cycles of 40 s at 94 °C, 30 s at 58 °C, 40 s at 72 °C, and finally 10 min at 72 °C for complete polymerization. Then the 5′ end and 3′ products were obtained. The two products were used as the template, and the second round of PCR was performed with the same components and conditions as the first PCR reaction except the two inner primers were used.

In Situ Hybridization (27). Nonradioactive in situ hybridization was performed on paraffin sections of mantle tissues of *P. fucata*. Ten probes covering specific regions of the new genes of the *P. fucata* mantle mRNA were provided by Invitrogen. In brief, slides were fixed in buffered, freshly prepared 4% paraformaldehyde solution for 10 min and then incubated in PBS containing 100 mM glycine and PBS containing 0.3% Triton X-100. After a short washing step with PBS, sections were digested for 30 min at 37 °C with TE buffer (100 mM Tris-HCl, 50 mM EDTA, pH 8.0) containing 1 mg/mL RNase-free proteinase K. Sections were again postfixed in 4% paraformaldehyde, washed in PBS, and treated in triethanolamine/acetic anhydride solution (0.1 M triethanolamine, pH 8.0, containing 0.25% acetic anhydride) on a rocking platform. After another PBS washing step, the slides were wiped dry around the tissue and laid out flat in airtight boxes on top of filter paper soaked in box buffer (4 × SSC, 50% formamide). Each section was covered with 20 mL of prehybridization buffer (50% formamide, 0.6 M NaCl, 10 mM Tris-HCl, pH 7.5, 1 mM EDTA, 50 mg/mL heparin, 10 mM dithiothreitol, 10% polyethylene glycol 8000, and Denhardt's solution). Seven milliliters of riboprobe in 40 mL of hybridization buffer was added to each section,

[1] Abbreviations: BMP-2, bone morphogenetic protein 2; bp, base pair; cDNA, complementary DNA; Dlx, distalless homeobox; dNTP, deoxynucleoside triphophate; DEPC, diethyl pyrocarbonate; EDTA, ethylenediaminetetraacetic acid; EtBr, ethidium bromide; GST, glutathione *S*-transferase; MEM, minimal essential medium; mRNA, messenger ribonucleic acid; oligo(dT), oligodeoxythymidylic acid; OPN, osteopontin; Osx, osterix; PBS, phosphate-buffered saline; *P. fucata*, *Pinctada fucata*; PFMG1, *P. fucata* mantle gene 1; RT-PCR, reverse transcription−polymerase chain reaction; Runx2, runt-related transcription factor 2; SDS, sodium dodecyl sulfate; SSH, suppression subtractive hybridization.

Table 1: Primers and Conditions Used for RT-PCR

gene	primers	PCR conditions	bp	ref
BMP-2	Fw: 5′-GTTCTGTCCCCAGTGACGAGTTT-3′ Rv: 5′-GTACAACATGGAGATTGCGCTGAG-3′	36 cycles, 95 °C for 1 min, 63 °C for 30 s, 72 °C for 1 min	708	*31*
osterix	Fw: 5′-GTCAAGAGTCTTAGCCAAACTC-3′ Rv: 5′-AATGATGTGAGGCCAGATGG-3′	25 cycles, 94 °C for 30 s, 58 °C for 30 s, 72 °C for 1 min	123	*32*
osteopontin	Fw: 5′-TCACCATTCGGATGAGTCTG-3′ Rv: 5′-ACTTGTGGCTCTGATGTTCC-3′	30 cycles, 95 °C for 1 min, 55 °C for 2 min, 72 °C for 1 min	437	*33*
β-actin	Fw: 5′-TGGACTTCGAGCAAGAGATG G-3′ Rv: 5′-ATCTCCTTCTGCATCCTGTCG-3′	23 cycles, 94 °C for 1 min, 62 °C for 45 s, 72 °C for 45 s	289	*34*

and the samples were incubated for 16 h at 52 °C. Hybridization was followed by two washes (10 min each) at room temperature in wash buffer (2 × SSC, 10 mM 2-mercaptoethanol, 1 mM EDTA). Slides were then immersed in RNase A solution (20 mg/mL) for 30 min at 37 °C and washed twice again in wash buffer at room temperature and then for 2 h in wash buffer containing 0.1 × SSC at 55 °C. Detection of the labeled and hybridized probe was performed using the DIG nucleic acid detection kit (Roche Molecular Biochemicals) by incubation for 30 min with alkaline phosphatase-labeled anti-digoxigenin Fab fragment (Roche Molecular Biochemicals, 1:700 in 0.1% goat serum, Tris-buffered saline at room temperature); the signal was developed using nitro blue tetrazolium/5-bromo-4-chloro-3-indolyl phosphate as substrate. The probes used for positive and negative controls were provided by the REMBRANDT RNA in situ hybridization kit (PanPath).

Multitissue RT-PCR (28). Total RNA was isolated from fresh adult *P. fucata* mantle, viscera, heart, lip, gill, adductor muscle, and viscera tissues using the RAN isolation kit (Gentra) according to instructions from the manufacturer. Reverse transcription was performed in the presence of 2 μg of RNA, 0.5 μg of oligo(dT)$_{18}$ primer, 10 mM dNTPs, 4 μL of 5 × reaction buffer, M-MuLV transcriptase (Sangon), RNase inhibitor, and RNase-free water in a total volume of 20 μL. A control reaction was performed in the absence of reverse transcriptase; control samples were otherwise treated identically. One microliter from the reverse-transcribed cDNA was used for each RT-PCR reaction. The reaction mixtures were also composed of 200 μM each of four deoxynucleotide triphosphates along with $MgCl_2$ (2 mM), 10 × PCR buffer, and 1.25 units of DNA polymerase (Sangon). This reaction mixture was then denatured (90 s at 95 °C) followed by 35 cycles of 40 s at 94 °C, 30 s at 58 °C, 40 s at 72 °C, and finally 5 min at 72 °C for complete polymerization.

Effect of GST-PFMG1 on $CaCO_3$ Crystallization. PFMG1 was cloned into PGEX-4T-2 (Amersham), was expressed in *Escherichia coli*, and was purified (data not shown). For crystallization experiments, saturated $CaCO_3$ solutions were prepared (*29*). Thirty to fifty milliliters of 100 mM $NaHCO_3$ was added to 120 mL of 40 mM $CaCl_2$ while stirring until the solution became turbid. Then the pH was adjusted to 8.2 with 1 M NaOH. The solution was centrifuged and filtered sterile. Fifty microliters of 1 mg/mL GST-PFMG1 in Tris buffer (pH 8.2) was added to 150 mL of the saturated solution on a glass plate. As two negative controls, buffer solutions with and without 1 mg/mL GST were used. The positive control was buffer solution with 1 mg/mL proteins extracted from nacre. A Leica DMIRB microscope was used for the morphological observation of the induced crystals.

Cell Culture. A robustly mineralizing subclone of the MC3T3-E1 cell line that has been previously described was used in this study (*30*). Cells were seeded at 1×10^5 cells/cm^2 in six-well plates for transfection and RT-PCR analyses. Cells were maintained in α-minimal essential medium (α-MEM) (GIBCO) with 10% FBS (Hyclone), 100 μg/mL streptomycin, and 100 units/mL penicillin. Starting at 90% confluency (typically day 3; day 0 = plating day), the culture medium was supplemented with 50 μg/mL ascorbic acid (Sigma) and 10 mM β-glycerophosphate (Sigma) to support differentiation and mineralization. The cultures were maintained at 37 °C in a humidified 5% CO_2 atmosphere.

Establishment of Transient MC3T3-E1 Cell Lines with Expression of PFMG1. The coding sequence of PFMG1 was amplified by RT-PCR from MC3T3-E1 with TaKaRa advantage 2 Taq DNA polymerase. Primers were designed with *Eco*RI and *Sal*I restriction sites in them, respectively. The amplified sequence was subcloned into the pUCm-T and then digested with *Eco*RI/*Sal*I (Promega). pcDNA.3.1/*myc*-HisA vector (Invitrogen) was used as the expression vector. The recombinant plasmid was named pcDNA.3.1/*myc*-HisA/PFMG1 (pcDNA/PFMG1). The expression vector pcDNA/PFMG1 was then transfected into MC3T3-E1. As a vector control, MC3T3-E1 cells were transfected with empty pcDNA.3.1/*myc*-HisA under the same conditions.

Immunoblot Analysis. Cells were harvested and washed twice with ice-cold PBS. The lysates were achieved with TEN-T buffer (150 mM NaCl, 10 mM Tris-HCl, pH 7.4, 5 mM EDTA pH 8.0, 1% Triton X-100, 1 mM PMSF, 2 μg/mL aprotinin) and then subjected to 10000*g* centrifugation at 4 °C for 10 min. Protein levels were quantified using bicinchoninic acid assay (Beyotime). Total proteins (50 μg/lane) were fractioned by 12.5% SDS−polyacrylamide gel electrophoresis for PFMG1 and β-actin protein and subsequently transferred to PVDF sheets. After blocking with TTBS (50 mM Tris-HCl, pH 7.4, 0.5 M NaCl, 0.05% Tween 20) containing 5% (w/v) skim milk, the sheets were incubated with c-Myc antibody (Santa Cruz) or with β-actin antibody (Sigma) at 4 °C overnight. Blots were then detected with an ECF western blotting kit (Amersham). The densities of sample bands were determined using a fluorescence scanner, Storm 860.

RT-PCR. Total RNA was isolated from treated cells using the Trizol reagent (Sangon) and immediately reverse-transcribed using oligo-p(dT)$_{18}$ primer and M-MuLV reverse transcriptase (Sangon) according to the manufacturer's protocol. Equal cDNA input amounts were determined by β-actin cDNA amplification. The primer sequences, annealing temperature, and cycle numbers for the amplification of each gene are listed in Table 1 (*31*−*34*). Then the PCR products were separated on 1.5% agarose gels, stained with

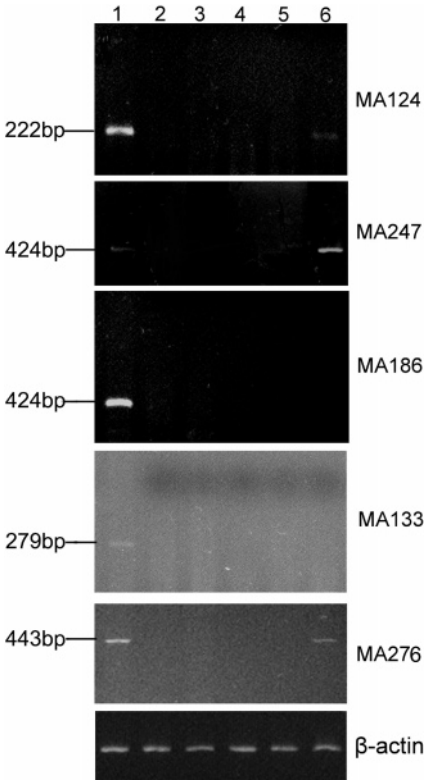

FIGURE 1: RT-PCR for analysis of novel EST expressions in *P. fucata*. Lanes: 1, mantle; 2, lip; 3, gill; 4, heart; 5, adductor muscle; 6, viscera. A housekeeping gene β-actin is included as a positive control.

EtBr, and photographed under UV illumination (Imagemaster VDS; Amersham).

RESULTS

Suppression Subtractive Hybridization Experiment. In order to identify genes that may be highly expressed in the mantle of *P. fucata*, we employed the SSH approach. The mRNAs from the mantle (tester) and other tissues (driver) of *P. fucata* were isolated. In the subsequent agarose electrophoresis, the different-sized subtracted cDNA fragments of the mantle sample were detected on 2% agarose/EtBr gel. The recombinant clones, including 768 clones from the previous subtraction and 384 clones from reverse subtraction, were identified by PCR and detected on 2% agarose/EtBr gel (data not shown). The results suggest that we obtained ESTs that are highly expressed in the mantle of *P. fucata*.

Identification of Partial Differentially Expressed ESTs in the Mantle by RT-PCR. We randomly selected five (MA124, MA247, MA186, MA133, MA276) from the identified ESTs, and they were examined and found indeed to be highly expressed in mantle tissue (Figure 1), which confirms the SSH method.

Reverse Northern Dot Blotting. In order to confirm differential expression of subtracted clones in mantle tissue, we detected the above 1152 clones by reverse Northern dot blotting (Figure 2). Total signal value homogenization was used for data analysis. We focused on the 768 clones that may have high expression in the mantle of *P. fucata* from former subtraction. The results show that 647 ESTs are highly expressed in the outer mantle of *P. fucata*. In

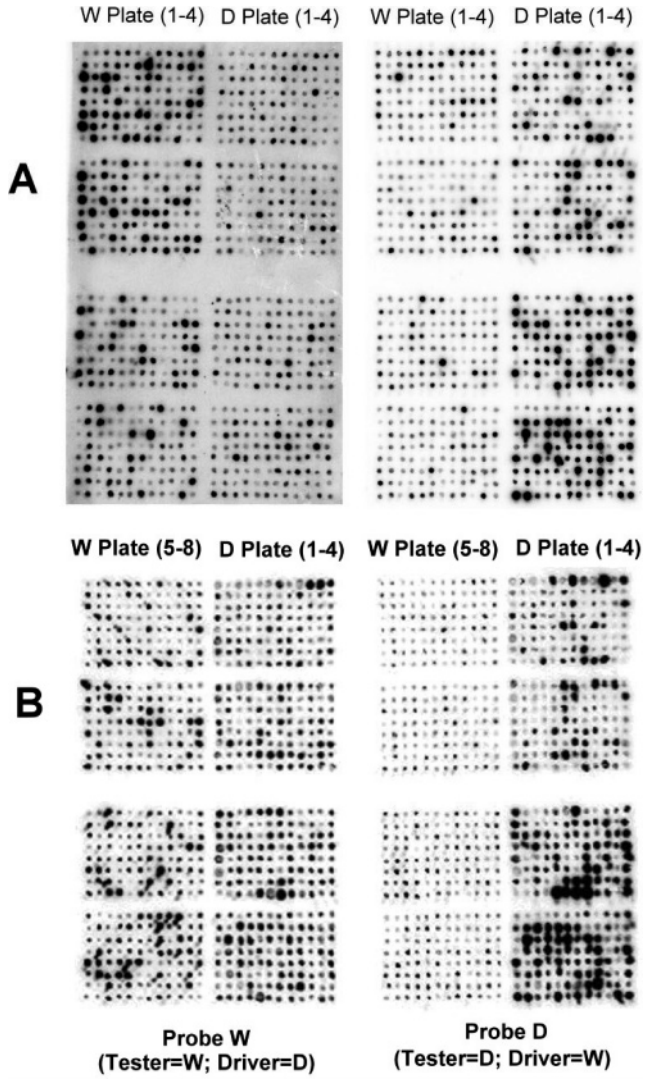

FIGURE 2: Reverse Northern dot blotting of PCR products from the SSH library: (A) membrane 1 (left) and membrane 2 (right); (B) membrane 3 (left) and membrane 4 (right); W plate (1−4) and W plate (5−8), 768 forward subtracted clones using probe W; D plate (1−4), 384 reverse subtracted clones using probe D as control.

membranes 1 and 2 there are 108 clones that are expressed 4 times higher in the mantle than in other tissues, and 34 of the clones are expressed 10 times higher (Figure 2A). In membranes 3 and 4 there are 101 clones that are expressed 4 times higher in the mantle than in other tissues, and 35 clones are expressed 10 times higher (Figure 2B).

Construction of a Mantle Tissue cDNA Library. Total RNA was isolated from 0.5 g of mantle tissue using Trizol reagent (GIBCO). The quality of total RNA was proven by $A_{260/280}$ absorbency and 2% agarose electrophoresis (data not shown). The products were digested by *Sfi*I and then fractionated by gel filtration through Sepharose spin-400. The cDNA products were then cloned into the pBluescript II SK vector. We obtained 1 mL of ligation product. Then we transformed *E. coli* DH5α using 1 μL of the ligation products to prove the library quality. There were 1020 clones on one plate and among them 9 blue clones, so the recombination rate was more than 99%, and the pool size was about 1.0×10^6. We sequenced 40 clones, blasted these sequences against the nr database, and found that 14 of them could be evaluated on integrality (*E* value less than 1e−09). Among the 14

Table 2: Molecular Cloning of Ten Novel Genes in the Mantle of *P. fucata*

gene name	GenBank accession no.	cDNA length (bp)	poly(A) tail site (bp)	signal peptide cleavage site (bp)	putative protein (aa)	homologous gene and conservative domain
PFMG1[a]	DQ104255	856	830−856	20 and 21	136	calcium-binding protein CBP-1
PFMG2	DQ104256	1239	1210−1239	not found	190	CH, calponin homology domain
PFMG3	DQ104257	639	611−639	23 and 24	121	similar to fertilin alpha-II
PFMG4	DQ104258	681	653−681	19 and 20	158	C1Q, complement component C1q domain
PFMG5	DQ104259	724	696−724	not found	108	not found
PFMG8	DQ104262	764	not found	21 and 22	223	not found
PFMG9	DQ116436	917	888−917	25 and 26	199	not found
PFMG10	DQ116437	764	not found	18 and 19	209	KAZAL, Kazal-type serine protease inhibitors and follistatin-like domains; OATP, organic anion transporter polypeptide (OATP) family
PFMG11	DQ116438	1089	1061−1089	16 and 17	191	articulin
PFMG12	DQ116439	831	802−831	21 and 22	158	KU domain, BPTI/Kunitz family of serine protease inhibitors

[a] PFMG = *P. fucata* mantle gene.

sequences, 4 were integrated and 2 were probably integrated. So the integrality rate is (4 + 2)/14 × 100% = 42.85%. The above test of the library quality proved that this library is eligible for the following gene cloning.

Cloning of the Novel Genes by Nested PCR. Primers were designed according to the EST sequence previously mentioned and were used in PCR assay with advantage 2 DNA polymerase (Clontech) and the mantle cDNA library of *P. fucata* as template. The PCR fragments were cloned into pUCm-T vectors and sequenced. Ten novel genes were identified by nested PCR and submitted to GenBank and were given accession numbers DQ104255−DQ104259, DQ104262, and DQ116436−DQ116439 (Table 2). Table 2 shows that eight novel genes have a signal peptide (PFMG1, PFMG3, PFMG4, and PFMG8−12). Most of these genes have a conserved domain or homologous genes, and the length is between 724 and 1239 bp. The sequence length of their encoding proteins is between 108 and 199 amino acids.

Sequencing and Analysis. PFMG1 has a high homology (40%) with *Onchocerca volvulus* calcium-binding protein CBP-1. On the basis of this, we think that PFMG1 may be a calcium-binding protein, so it could be responsible for the nucleation of calcium compounds and may participate in nacre formation (Figure 3B). The deduced protein is composed of 136 amino acids and has an estimated molecular mass of 15.7 kDa with an isoelectric point of 7.69. A search for the protein domain in the PROSITE database revealed two EF-hand calcium-binding domains from the 81st to the 93rd amino acid and from the 98th to the 133rd amino acid in the deduced amino acid sequence (Figure 3A).

In Situ Hybridization. To confirm the high expression of PFMG1 mRNA in mantle tissue, we used paraffin-embedded mantle sections of the pearl oyster (*P. fucata*). Strong mRNA hybridization signals were detected in the cells of the mantle. The positive control showed that hybridization signals were distributed throughout the mantle section, while no hybridization signal was detected in the negative control (Figure 4). The probes used for positive and negative control were provided by the REMBRANDT RNA in situ hybridization kit (PanPath).

Identification of Partial Differentially Expressed PFMG1 in the Mantle by RT-PCR. PFMG1 was examined and found indeed to be highly expressed in mantle tissue (Figure 5).

Effect of GST-PFMG1 on $CaCO_3$ Crystallization. In the crystallization experiment, crystals formed in the presence

FIGURE 3: Sequence analysis. The initial codon and the stop codon are in blue letters, and the two EF-hand domains are in red letters (A). The sequences were analyzed using Blast (NCBI) software, and the homology was compared with the sequences in GenBank. PFMG1 has a high homology (40%) with *O. volvulus* calcium-binding protein CBP-1 (B).

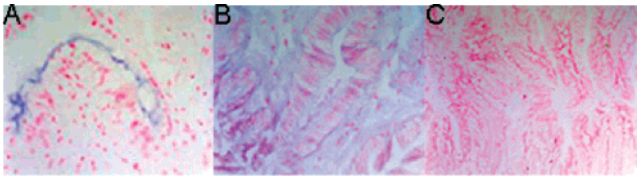

FIGURE 4: In situ hybridization of PFMG1 mRNA in the mantle of *P. fucata*. The PFMG1 transcript was detected in the mantle paraffin section with the digoxigenin-labeled RNA probe. A strong hybridization signal is present in the outer epithelia of the mantle (purple staining). (A) PFMG1; (B) positive control; (C) negative control. Original magnification: 400×.

of GST-PFMG1 (Figure 6C) exhibited morphological changes compared to crystals formed in the two negative control solutions (Figure 6A,B), while crystals formed under the

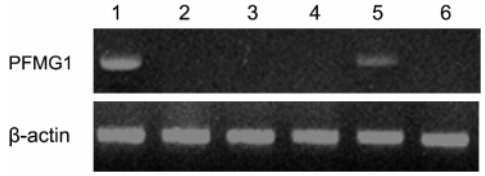

FIGURE 5: RT-PCR for analysis of PFMG1 expression in *P. fucata*. Lanes: 1, mantle; 2, lip; 3, gill; 4, heart; 5, adductor muscle; 6, viscera. A housekeeping gene β-actin is included as a positive control.

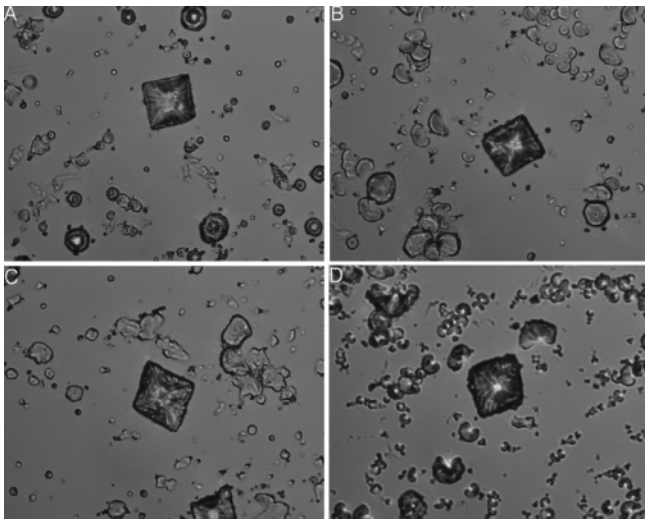

FIGURE 6: Light microscopic images of crystals grown in a saturated $CaCO_3$ solution. (A−D) Crystals formed in the presence of Tris solution, GST, GST-PFMG1, and proteins extracted from nacre, respectively (400× magnification). The crystals in (A) and (B) are cubic, while many are rhombic in (C) and (D).

treatment of Tris or GST showed no difference from the natural $CaCO_3$ crystals (data not shown). The morphological changes are almost the same in the presence of GST-PFMG1 (Figure 6C) and proteins extracted from nacre (Figure 6D). Crystals formed in the negative control solution (Figure 6A,B) are cubic, while in the solution with GST-PFMG1 (Figure 6C) and proteins extracted from nacre (Figure 6D), many crystals are rhombic. These results indicated that PFMG1 affected the nucleation and growth of $CaCO_3$ crystals.

Transient Expression of PFMG1 in MC3T3-E1 Cells To Investigate the Impact of PFMG1 Expression on Osteoblastic Function. MC3T3-E1 cells transduced with pcDNA/PFMG1 were cultured and compared to cells transduced with the empty pcDNA vector. After 24 h from transfection, cells were collected and analyzed if PFMG1 protein could be expressed. As Figure 7A showed, pcDNA/PFMG1 transfected cells expressed PFMG1 protein with a myc tag at 19 kDa, which could be examined by c-myc antibody (recognized c-Myc amino acids 408−439), while vector alone transfected cells expressed no protein at 19 kDa (Figure 7A).

BMP-2, Osteopontin, and Osterix Were Upregulated in PFMG1 Expression Osteoblasts. It was examined whether expression of PFMG1 affected the expression of marker genes of the osteoblast phenotype. For this purpose we performed RT-PCR using primers for the housekeeping gene β-actin. The osteoblast markers BMP-2, osteopontin (OPN), and osterix (Osx) were remarkably increased by expression of PFMG1 (Figure 7B).

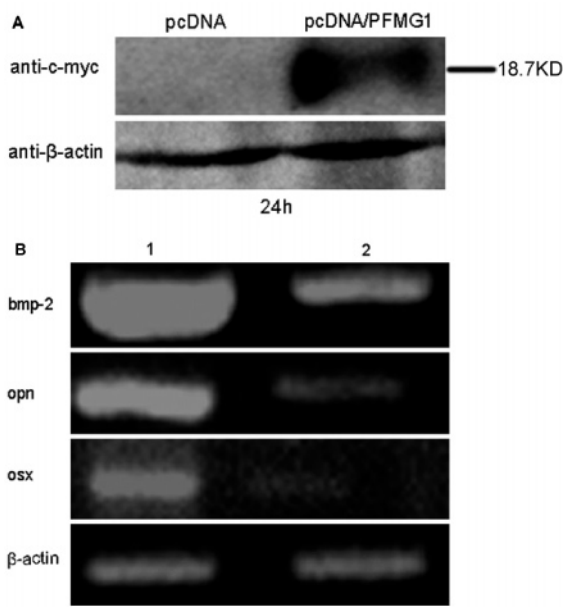

FIGURE 7: (A) Transient expression of PFMG1 in MC3T3-E1 cells. Immunoblot analysis of PFMG1. Total cell lysate isolated from vector-transfected or stably transfected pcDNA/PFMG1 clones were analyzed for PFMG1 protein by immunoblot analysis using an anti-c-Myc antibody (1:500) recognizing human c-Myc (amino acids 408−439) or an anti-β-actin monoclonal antibody (1:500000). Western blot analysis of cells was performed 24 h after transfection. Lanes: pcDNA, vector alone transfected cells; pcDNA/PFMG1, pcDNA/PFMG1 expression vector transfected cells. (B) Effects on the mRNA expression of osteoblast marker genes by expression of PFMG1 cells. 90% confluent osteoblasts were incubated for 6 days, and RNA was extracted. 1 mg of total RNA was reverse-transcribed, and the equivalent of 0.1 μg was subjected to PCR using primer pairs and conditions as described in Table 1. Similar results were observed in three independent experiments. Lanes: 1, expression of PFMG cells; 2, cells transfected with empty pcDNA vector.

DISCUSSION

Research concerning biomineralization of the pearl shell has mainly focused on the identification of certain proteins or peptides involved in mineralization. Due to the limitations of experimental methods and the small quantity of purified proteins, the study on the function of relative proteins still remains hypothetical. The results of previous studies have revealed that calcium carbonate crystals are constructed under the control of multiproteins, not a single protein. Therefore, understanding the mechanisms of biomineralization of pearl shells depends on not only the cloning and study of genes encoding the pearl matrix proteins but also the study of genes involved in the regulation of mineralization.

Identifying the functional genes involved in nacre biomineralization will not only be beneficial for further studies on the molecular mechanism of nacre biomineralization but may also boost the output and quality of pearls through bioengineering.

Suppression subtractive hybridization is a powerful technique that enables researchers to compare two populations of mRNA and obtain clones of genes that are expressed in one population but not in the other. Furthermore, this method can prevent undesirable amplification while enrichment of target molecules proceeds. This study is the first time that this method has been performed on *P. fucata*. As a result, 768 clones with high expression in the mantle were obtained,

of which 647 ESTs were confirmed in the subsequent reverse Northern dot blotting (Figure 2). On the basis of the ESTs and the mantle cDNA library, we identified ten novel genes by nested PCR (Table 2).

Five randomly selected ESTs (MA124, MA247, MA186, MA133, MA276) from the ESTs identified by SSH were examined and found indeed to be highly expressed in mantle tissue (Figure 1), which confirms the SSH method. Three of the five examined ESTs (MA124, MA247, MA276) are found also to be positive in the viscera sample (Figure 1). This may be because, in the SSH process, the viscera and other tissues were together used as the driver, so the concentration of the three ESTs in viscera was diluted. Therefore, in the multitissue RT-PCR, the three ESTs became positive when examined in the viscera sample (Figure 1).

PFMG1 has a high homology (40%) with *O. volvulus* calcium-binding protein CBP-1 (Figure 3). On the basis of this we think that PFMG1 may be a calcium-binding protein. PFMG1 has two EF-hand calcium-binding domains from the 81st to the 93rd amino acid and from the 98th to the 133rd amino acid in the deduced amino acid sequence. So it could be responsible for the nucleation of calcium compounds and may participate in nacre formation.

The results of multitissue RT-PCR and in situ hybridization confirm that PFMG1 is indeed highly expressed in mantle tissue, a tissue which is responsible for the secrecy of many organic matrixes and is vital to pearl formation. And the results confirm the SSH method (Figures 4 and 5). It is also interesting that the PFMG1 is expressed in the adductor muscle. The EF-hand proteins have been found and characterized in a wide range of living organisms including bacteria, plants, and animals (*35*) and have a wide range of functions including calcium buffering, transport, signal transduction (*36*), and muscle contraction (*37*). The PFMG1 protein may be involved in signal transduction during this process, leading to the biomineralization of nacre when it binds Ca^{2+}.

The results of GST-PFMG1 on $CaCO_3$ crystallization indicated that PFMG1 affected the nucleation and growth of $CaCO_3$ crystals. PFMG1 may play a significant role in the biomineralization process of pearl formation (Figure 6).

It is observed in PFMG1 expression osteoblasts that a significant upregulation of BMP-2, OPN, and Osx gene transcripts relative to normal cells occurs (Figure 7). These markers are considered to be highly predictive of the differentiated osteoblast phenotype. But the transcriptional regulation of these genes is not well characterized. BMPs were discovered for their ability to induce cartilage and bone formation from nonskeletal mesodermal cells and are now of considerable interest as therapeutic agents for healing fractures and periodontal bone defects and for inducing bone growth around implants and prostheses (*38*). BMP-2 is accumulated in the extracellular matrix (ECM) and is able to stimulate ectopic bone formation in vivo and osteoblastic differentiation in vitro. It stimulates the expression of three osteogenic master transcription factors: Runx2, Dlx5, and Osx (*39*). Osx was commonly stimulated in osteogenic and nonosteogenic cells in response to BMP signaling. Our results showed that expression of PFMG1 remarkably increased mRNA of BMP-2, Osx, and OPN. This suggested that the effects of PFMG1 expression on osteoblast differentiation and mineralization might be through BMP signaling and the expressed PFMG1 might be an upstream factor of BMP-2. How the PFMG1 protein functions in the BMP pathway will be further characterized in our study.

So that PFMG1 can be closely involved in the nacre biomineralization, the SSH method can pave the way for the bulk cloning and characterization of new genes involved in biomineralization in *P. fucata* and may accelerate the research on the mechanism of pearl formation.

REFERENCES

1. Westbroek, P., and Marin, F. (1998) A marriage of bone and nacre, *Nature 392*, 861−862.
2. Boskey, A. (1998) Biomineralization: conflicts, challenges, and opportunities, *J. Cell. Biochem., Suppl.* 30−31, 83−91.
3. Lowenstam, H. A., and Weiner, S. (1989) *On Biomineralization*, Oxford University Press, New York.
4. Lowenstam, H. A. (1981) Minerals formed by organisms, *Science 211*, 1126−1131.
5. Simkiss, K., and Allemand, D. (1993) in *Biomineralization*, 93rd ed., Musee Oceanographique, Monaco.
6. Krampitz, G., and Graser, G. (1988) Molecular mechanism of biomineralization in the formation of calcified shells, *Angew. Chem. 27*, 1145−1156.
7. Addadi, L., and Weiner, S. (1997) Biomineralization: A pavement of pearl, *Nature 389*, 912−915.
8. Aizenberg, J., Muller, D. A., Grazul, J. L., and Hamann, D. R. (2003) Direct fabrication of large micropatterned single crystals, *Science 299*, 1205−1208.
9. Belcher, A. M., Wu, X. H., Christensen, R. J., Hansma, P. K., Stucky, G. D., and Morse, D. E. (1996) Control of crystal phase switching and orientation by soluble mollusc-shell proteins, *Nature 381*, 56−58.
10. Mann, S., Heywood, B. R., Rajam, S., and Birchall, J. D. (1988) Controlled crystallization of $CaCO_3$ under stearic acid monolayers, *Nature 334*, 692−695.
11. Falini, G. S., Albeck, S., Wiener, S., and Addadi, L. (1996) Control of aragonite or calcite polymorphism by mollusk shell macromolecules, *Science 271*, 67−69.
12. Mount, A. S., Wheeler, A. P., Paradkar, R. P., and Snider, D. (2004) Hemocyte-mediated shell mineralization in the eastern oyster, *Science 304*, 297−300.
13. Sudo, S., Fujikawa, T., Nagakura, T., Ohkubo, T., Sakaguchi, K., Tanaka, M., and Nakashima, K. (1997) Structures of mollusc shell framework proteins, *Nature 387*, 563−564.
14. Zhang, Y., Xie, L. P., Meng, Q. X., Jiang, T., Pu, R., Chen, L., and Zhang, R. Q. (2003) A novel matrix protein participating in the nacre framework formation of pearl oyster, *Pinctada fucata*, *Comp. Biochem. Physiol., Part B: Biochem. Mol. Biol. 135*, 565−573.
15. Samata, T., Hayashi, N., Kono, M., Hasegawa, K., Horita, C., and Akera, S. (1999) A new matrix protein family related to the nacreous layer formation of *Pinctada fucata*, *FEBS Lett. 462*, 225−229.
16. Miyamoto, H., Miyashita, T., Okushima, M., Nakano, S., Morita, T., and Matsushiro, A. (1996) A carbonic anhydrase from the nacreous layer in oyster pearls, *Proc. Natl. Acad. Sci. U.S.A. 93*, 9657−9660.
17. Miyashita, T., Takagi, R., Okushima, M., Nakano, S., Miyamoto, H., Nishikawa, E., and Matsushiro, A. (2000) Complementary DNA cloning and characterization of pearlin, a new class of matrix protein in the nacreous layer of oyster pearls, *Mar. Biotechnol. 2*, 409−418.
18. Zhang, Y., Huang, J., Meng, Q. X., Jiang, T., Xie, L. P., Wang, Z., and Zhang, R. Q. (2004) Molecular cloning and expression of a pearl oyster (*Pinctada fucata*) homologue of mammalian putative tumor suppressor QM, *Mar. Biotechnol. 6*, 8−16.
19. Green, H., Canfield, A. E., Hillarby, M. C., Grant, M. E., Boot-Handford, R. P., Freemont, A. J., and Wallis, G. A. (2000) The ribosomal protein QM is expressed differentially during vertebrate endochondral bone development, *J. Bone Miner. Res. 15*, 1066−1075.
20. Li, S., Xie, L. P., Zhang, C., Zhang, Y., Gu, M., and Zhang, R. Q. (2004) Cloning and expression of a pivotal calcium metabolism regulator: calmodulin involved in shell formation from pearl

oyster (*Pinctada fucata*), *Comp. Biochem. Physiol., Part B: Biochem. Mol. Biol. 138*, 235−243.
21. Suzuki, M., Murayama, E., Inoue, H., Ozaki, N., Tohse, H., Kogure, T., and Nagasawa, H. (2004) Characterization of prismalin-14, a novel matrix protein from the prismatic layer of the Japanese pearl oyster (*Pinctada fucata*), *J. Biochem. 382*, 205−213.
22. Tsukamoto, D., Sarashina, I., and Endo, K. (2004) Structure and expression of an unusually acidic matrix protein of pearl oyster shells, *Biochem. Biophys. Res. Commun. 320*, 1175−1180.
23. Zhang, Y., Meng, Q. X., Jiang, T. M., Wang, H. Z., Xie, L. P., and Zhang, R. Q. (2003) A novel ferritin subunit involved in shell formation from the pearl oyster (*Pinctada fucata*), *Comp. Biochem. Physiol., Part B: Biochem. Mol. Biol. 135*, 43−54.
24. Chen, L., Xie, L. P., Dai, Y., Xiong, X., Fan, W., and Zhang, R. Q. (2004) Cloning and characterization of an mRNA encoding a novel G protein alpha-subunit abundant in mantle and gill of pearl oyster *Pinctada fucata*, *Comp. Biochem. Physiol., Part B: Biochem. Mol. Biol. 139*, 669−679.
25. Diachenko, L., Lau, Y. F. C., Campbell, A., Chenchik, A., Moqadam, F., Huang, B., Lukyanov, K., Lukyanov, S., Gurskaya, N., Sverdlov, E., and Siebert, P. (1996) Suppression subtractive hybridization: A method for generating differentially regulated or tissue-specific cDNA probes and libraries, *Proc. Natl. Acad. Sci. U.S.A. 93*, 6025−6030.
26. Robichaud, G. A., Nardini, M., Laflamme, M., Cuperlovic-Culf, M., and Ouellette, R. J. (2004) Differential amplification of intron-containing transcripts reveals long term potentiation-associated up-regulation of specific Pde10A phosphodiesterase splice variants, *J. Biol. Chem. 279*, 49956−49963.
27. Liu, S. F., Lu, G. X., Liu, G., Xing, X. W., Li, L. Y., and Wang, Z. (2004) Cloning of a full-length cDNA of human testis-specific spermatogenic cell apoptosis inhibitor TSARG2 as a candidate oncogene, *Biochem. Biophys. Res. Commun. 319*, 32−40.
28. O'Connor, V., Genin, A., Davis, S., Karishma, K. K., Doyere, V., De Zeeuw, C. I., Sanger, G., Hunt, S. P., Richter-Levin, G., Mallet, J., Laroche, S., Bliss, T. V., and French, P. J. (2004) Differential amplification of intron-containing transcripts reveals long term potentiation-associated up-regulation of specific Pde10A phosphodiesterase splice variants, *J. Biol. Chem. 279*, 15841−15849.
29. Weiss, I. M., Kaufmann, S., Mann, K., and Fritz, M. (2000) Purification and characterization of perlucin and perlustrin, two new proteins from the shell of the mollusc *Haliotis laevigata*, *Biochem. Biophys. Res. Commun. 267*, 17−21.
30. Smith, E., Redman, R. A., Logg, C. R., Coetzee, G. A., Kasahara, N., and Frenkel, B. (2000) Glucocorticoids inhibit developmental stage-specific osteoblast cell cycle. Dissociation of cyclin A-cyclin-dependent kinase 2 from E2F4-p130 complexes, *J. Biol. Chem. 275*, 19992−20001.
31. Luppen, C. A., Smith, E., Spevak, L., Boskey, A. L., and Frenkel, B. (2003) Bone morphogenetic protein-2 restores mineralization in glucocorticoid-inhibited MC3T3−E1 osteoblast cultures, *J. Bone Miner. Res. 18*, 1186−1197.
32. Yang, J. H., Zhao, L., Yang, S., Wu, S. Q., Zhang, J., and Zhu, T. H. (2003) Expression of recombinant human BMP-6 in *Escherichia coli* and its purification and bioassay in vitro, *J. Chin. Biotechnol. 19*, 556−560.
33. Chackalaparampil, I., Peri, A., Nemir, M., Mckee, M. D., Lin, P. H., Mukherjee, B. B., and Mukherjee, A. B. (1996) Cells in vivo and in vitro from osteopetrotic mice homozygous for c-src disruption show suppression of synthesis of osteopontin, a multifunctional extracellular matrix protein, *Oncogene 12*, 1457−1467.
34. Wu, R. C., Wang, Z., Liu, M. J., Chen, D. F., and Yue, X. S. (2004) beta2-integrins mediate a novel form of chemoresistance in cycloheximide-induced U937 apoptosis, *Cell. Mol. Life Sci. 61*, 2071−2082.
35. Kawasaki, H., Nakayama, S., and Kretsinger, R. H. (1998) Classification and evolution of EF-hand proteins, *Biometals 11*, 277−295.
36. Skelton, N. J., Kordel, J., Akke, M., Forsen, S., and Chazin, W. J. (1994) Signal transduction versus buffering activity in Ca(2+)-binding proteins, *Nat. Struct. Biol. 1*, 239−245.
37. Holmes, K. C. (1996) Muscle proteins—their actions and interactions, *Curr. Opin. Struct. Biol. 6*, 781−789.
38. Linkhart, T. A., Mohan, S., and Baylink, D. J. (1996) Growth factors for bone growth and repair: IGF, TGF beta and BMP, *Bone (Suppl.) 19*, 1S−12S.
39. Lee, M. H., Kwon, T. G., Park, H. S., Wozney, J. M., and Ryooa, H. M. (2003) BMP-2-induced osterix expression is mediated by Dlx5 but is independent of Runx2, *Biochem. Biophys. Res. Commun. 309*, 689−694.

BI061881A